Photooxidation of RPE lipofuscin bisretinoids enhances fluorescence intensity

So Ra Kim [a,1], Young Pyo Jang [a,2], Janet R. Sparrow [a,b,*]

[a] Department of Ophthalmology, Columbia University, 630 W 168th Street, New York, NY 10032, United States
[b] Department of Pathology and Cell Biology, Columbia University, 630 W 168th Street, New York, NY 10032, United States

ARTICLE INFO

ABSTRACT

Light-related cycling of chemically reactive vitamin A aldehyde leads to the formation autofluorescent bis-retinoid pigments that accumulate as lipofuscin in retinal pigment epithelial cells. The amassing of these diretinoid compounds is implicated in the pathogenesis of age-related macular degeneration and in some inherited forms of retinal degeneration. For all of these fluorophores, extended conjugation systems confer absorbance maxima in the visible spectrum. We report that an increase in fluorescence emission can accompany photoxidation of the bisretinoids A2E and all-*trans*-retinal dimer. These findings are relevant to the quantification of RPE lipofuscin based on inference from fluorescence intensity.

© 2009 Elsevier Ltd. All rights reserved.

1. Introduction

Laser scanning ophthalmoscopic imaging and non-invasive spectrophotometry demonstrates that the fundus of the retina exhibits an intrinsic autofluorescence that emanates from the lipofuscin deposited in retinal pigment epithelial (RPE) cells (Delori, Dorey, et al., 1995; von Ruckmann, Fitzke, & Bird, 1997). The pigments that constitute the lipofuscin of RPE cells accumulate with age and form in particular abundance in some retinal disorders such as autosomal recessive Stargardt disease (STGD1) (Delori, Staurenghi, et al., 1995). Excessive accumulation of lipofuscin is considered to be the cause of RPE atrophy in STGD1 (Radu et al., 2005) and studies of fundus autofluorescence have shown that areas of intense fundus autofluorescence in patients with age-related macular degeneration correspond to sites of reduced scotopic sensitivity and are prone to atrophy (Holz et al., 1999; Schmitz-Valckenberg et al., 2004; Scholl, Bellmann, Dandekar, Bird, & Fitzke, 2004). Moreover, monitoring of the autofluorescence of the fundus provides information valuable for diagnosing and anticipating the course of atrophic macular degeneration, both juvenile (STGD1)

and age-related atrophic forms (Lois, Holder, Bunce, Fitzke, & Bird, 2001; Lois et al., 2002; von Rückmann, Fitzke, & Bird, 1997).

When measured at the fundus, the autofluorescence of RPE lipofuscin is excited by short-wavelength light in the blue region of the spectrum and has a broad emission centered at approximately 610 nm (Delori, Dorey, et al., 1995; Delori, Goger, & Dorey, 2001). The extended conjugation system within the polyene structure and aromatic ring of the bis-retinoid pigments of RPE lipofuscin, provide the structural features that confer excitation and emission wavelengths in the visible range of the spectrum. Prominent amongst these lipofuscin chromophores are the pyridinium bis-retinoid compounds A2E (Fig. 1), (Eldred & Katz, 1988; Eldred & Lasky, 1993; Parish, Hashimoto, Nakanishi, Dillon, & Sparrow, 1998; Sakai, Decatur, Nakanishi, & Eldred, 1996), the C13–C14 Z-isomer of A2E (isoA2E) (Fig. 1) and other less abundant isomers having cis-double bonds at other positions (Ben-Shabat, Parish, et al., 2002; Parish et al., 1998). Of additional significance are bis-retinoid constituents of RPE lipofuscin that constitute the all-*trans*-retinal dimer series (Fig. 1) including all-*trans*-retinal dimer and the related conjugates all-*trans*-retinal dimer-phosphatidyletha-nolamine (all-*trans*-retinal dimer-PE) and all-*trans*-retinal dimer-ethanolamine (all-*trans*-retinal dimer-E) (Fishkin, Sparrow, Allik-mets, & Nakanishi, 2005; Kim, Jang, et al., 2007). The most recently identified members of the bisretinoid family are A2-dihydropyri-dine-phosphatidylethanolamine (A2-DHP-PE) and A2-dihydropyri-dine-ethanolamine, pigments that present with a dihydropyridine head-group (Wu, Fishkin, Pande, Pande, & Sparrow, 2009). A structural feature common to all of these bis-retinoid compounds is a central six-sided ring from which extend two side-arms, a long

* Corresponding author. Address: Department of Ophthalmology, Columbia University, 630 W 168th Street, New York, NY 10032, United States. Fax: +1 212 305 9638.
  E-mail address: jrs88@columbia.edu (J.R. Sparrow).
[1] Present address: Department of Visual Optics, Seoul National University of Technology, Seoul 139-743, South Korea.
[2] Present address: Kyung Hee East-West Pharmaceutical Research Institute, College of Pharmacy, Kyung Hee University, Seoul 130-701, Korea.
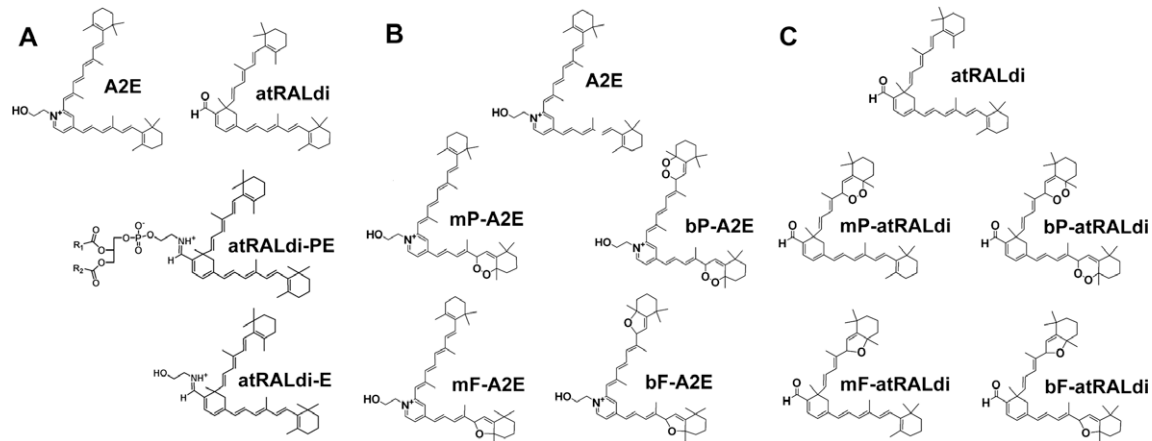
Fig. 1. The structures of some bisretinoid constituents of RPE lipofuscin. (A) A2E, all-*trans*-retinal dimer (atRALdi), all-*trans*-retinal dimer-PE (atRALdi-PE), and all-*trans*-retinal dimer-E (atRALdi-E). (B) A2E and photooxidized forms of A2E: monoperoxy-A2E (mP-A2E), bisperoxy-A2E (bP-A2E), monofurano-A2E (mF-A2E) and bisfurano-A2E (bF-A2E). (C) All-*trans*-retinal dimer (atRALdi) and photoxidized forms of all-*trans*-retinal dimer: monoperoxy-all-*trans*-retinal dimer (mP-atRALdi), bisperoxy-all-*trans*-retinal dimer (bP-atRALdi), mono-furano-all-*trans*-retinal dimer (mF-atRALdi) and bisfurano-all-*trans*-retinal dimer (bF-atRALdi).

arm and short arm, each of which is derived from a molecule of all-*trans*-retinal (Fig. 1).

The pigment all-*trans*-retinal dimer forms when molecules of all-*trans*-retinal, rather than undergoing reduction to retinol, condense to form an aldehyde-bearing dimer (all-*trans*-retinal dimer) within photoreceptor outer segments (Fishkin et al., 2005; Kim, Jang, et al., 2007). Subsequent reaction with phosphatidylethanolamine generates all-*trans*-retinal dimer-phosphatidylethanolamine (all-*trans*-retinal dimer-PE), a conjugate containing a Schiff base linkage that is protonated. The protonation state of the imine nitrogen is pH-dependent. Phosphate hydrolysis of all-*trans*-retinal dimer-PE generates all-*trans*-retinal dimer-E. The synthesis of A2E, on the other hand, begins when a molecule of all-*trans*-retinal reacts with PE (Liu, Itagaki, Ben-Shabat, Nakanishi, & Sparrow, 2000) to form an initial Schiff base conjugate (*N*-retinylidene-PE, NRPE). Reaction of NRPE with a second all-*trans*-retinal leads to the formation of a dihydropyridinium compound (dihydropyridinium-A2PE) that undergoes automatic oxidative aromatization with elimination of two hydrogens to yield A2PE (Ben-Shabat, Parish, et al., 2002; Kim, He, et al., 2007; Liu et al., 2000; Parish et al., 1998). Alternatively, dihydropyridinium-A2PE can eliminate one hydrogen to form the bisretinoid A2-DHP-PE (Wu et al., 2009).

It is well known that when A2E and all-*trans*-retinal dimer are irradiated with short-wavelength light (e.g. 430 nm) these compounds can serve as photosensitizers generating various reactive forms of oxygen that then add at carbon–carbon double bonds along the side-arms of the molecules (Ben-Shabat, Itagaki, et al., 2002; Jang, Matsuda, Itagaki, Nakanishi, & Sparrow, 2005; Kim, Jockusch, Itagaki, Turro, & Sparrow, 2008; Kim, Jang, et al., 2007; Sparrow, Nakanishi, & Parish, 2000; Sparrow et al., 2002). In the case of both A2E and all-*trans*-retinal dimer the initial oxidation always occurs at the distal end of the short arm (5,6 double bond), the most electron-rich region of the molecule (Jang et al., 2005; Kim, Jang, et al., 2007). The oxygen-containing moieties that form within photooxidized-A2E and all-*trans*-retinal dimer include endoperoxides, epoxides and furanoid moieties, the structures of which have been corroborated by mass spectrometry and HSQC-NMR spectroscopy (Jang et al., 2005; Kim, Jang, et al., 2007). These oxidized forms have also been identified in hydrophobic extracts of human RPE and Abca4$^{-/-}$ mouse eyecups and likely account for the adverse effects of A2E photoreactivity (Jang et al., 2005; Kim, Jang, et al., 2007). All-*trans*-retinal dimer generates singlet oxygen with greater efficiency than A2E and the all-*trans*-retinal dimer series of compounds are also more efficient quenchers of singlet oxygen (Kim, Jang, et al., 2007).

Here we have compared the fluorescence emission properties of A2E, all-*trans*-retinal dimer, all-*trans*-retinal dimer-PE, and all-*trans*-retinal dimer-E and we report that fluorescence intensity can increase with photooxidation.

2. Material and methods

2.1. Reagents

All-*trans*-retinal, ethanolamine, trifluoroacetic acid (TFA), formic acid and *meta*-chloroperoxy-benzoic acid (MCPBA) were purchased from Aldrich Chemical Company, Inc. (Milwaukee, WI); acetonitrile was purchased from Fisher (Fair Lawn, NJ). All other chemicals were obtained from Sigma–Aldrich (St. Louis, MO).

2.2. Human tissue and mice

Human donor eyes were obtained from the National Disease Research Interchange (Philadelphia, PA) and RPE/choroid was isolated. *Abca4/Abcr*$^{-/-}$ and *Abca4/Abcr*$^{+/+}$ mice (albino) homozygous for Rpe65 Leu-450 were generated, genotyped and housed in a 12-h-on/12-h-off light cycle as previously reported (Kim et al., 2004; Wu et al., 2009). For Rpe65 genotyping, digestion of the 545-bp PCR product with *Mwo*I restriction enzyme (New England Biolabs), yielded 180- and 365-bp fragments in mice homozygous for Rpe65 Leu-450.

2.3. Synthesis of compounds

A2E was synthesized from all-*trans*-retinal and ethanolamine as described previously (Parish et al., 1998). All-*trans*-retinal dimer, all-*trans*-retinal dimer-E, and all-*trans*-retinal dimer-PE (Fig. 1) were synthesized as formerly published (Fishkin et al., 2005). The structures of synthesized standards of A2E/isoA2E and all-*trans*-retinal dimer, all-*trans*-retinal dimer-E, and all-*trans*-retinal dimer-PE have been corroborated (Fishkin, Pescitelli, Sparrow, Nakanishi, & Berova, 2004; Fishkin et al., 2005; Liu et al., 2000; Parish et al., 1998; Sakai et al., 1996). The endoperoxide of 1,4-dimethylnaphthalene was synthesized as described (Turro, Chow, & Rigaudyo, 1981). A2E and all-*trans*-retinal dimer were incubated with endoperoxide of 1,4-dimethylnaphthalene to generate peroxy-A2E and peroxy – all-*trans*-retinal dimer (Jang et al., 2005). Similarly, incubation with MCPBA produced furano-A2E and furano – all-*trans*-retinal dimer (Kim, Jang,

et al., 2007). These oxidized forms of A2E and all-*trans*-retinal dimer are produced in the eye by photooxidation (Jang et al., 2005; Kim, Jang, et al., 2007). All of the above compounds were purified by HPLC.

2.4. Tissue extraction and HPLC analysis

Isolated human RPE/choroid and murine posterior eye cups were pooled and homogenized in buffer using a tissue grinder. An equal volume of a mixture of chloroform/methanol (1:1) was added and the sample was extracted three times by addition of chloroform and then centrifuged at 1000g for 2 min. After passage through a reversed phase (C8 Sep-Pak, Millipore) cartridge with 0.1% TFA in methanol, the extract was concentrated by evaporation of solvent under gas and was redissolved in 50% methanolic chloroform.

An Alliance system (Waters, Corp, Milford, MA) equipped with 2695 Separation Module, 2996 Photodiode Array Detector, 2475 Multi λ Fluorescence Detector and operating with Empower® software was used for HPLC analysis. An Atlantis® dC18 column (3 μm, 4.6 × 150 mm, Waters, USA) and a Delta Pak® C4 column (5 μm, 3.9 × 150 mm, Waters, USA) were employed. For analysis of A2E, A2PE, all-*trans*-retinal dimer-PE and all-*trans*-retinal dimer-E, the following gradient of acetonitrile in water (with 0.1% trifluoroacetic acid) were used: (A) 0–5 min; 75% acetonitrile, flow rate, 0.8 ml/min; 5–20 min, 75–100% acetonitrile; flow rate, 0.8–1.2 ml/min; 20–30 min, 100% acetonitrile, flow rate, 1.2 ml/min with C4 column, and (B) 85–100% (0–15 min) acetonitrile; 100% acetonitrile (15–30 min) with a flow rate of 0.8 ml/min with C18 column.

For analysis of oxidized-A2E and oxidized all-*trans*-retinal dimer, the eye extracts were injected on a reverse-phase C18 column (4.6 mm × 150 mm; 3 m) and monitored at 430 nm by photo diode array. The gradient of acetonitrile in water (with 0.1% TFA) was 75–90% (0–30 min) acetonitrile; 90–100% acetonitrile (30–40 min); 100% acetonitrile (40–80 min) with a flow rate of 0.5 ml/min. HPLC injection volume was 10 μl. Quantification was carried out using the Empower® software to determine peak areas. Extraction and injection for HPLC were performed under dim red light.

2.5. Fluorescence spectroscopy

Fluorescence emission spectra were measured at room temperature on a SPEX Fluorolog-3 spectrometer FL3-22 (J.Y. Horiba, Edison, NJ) using quartz cuvettes with optical path lengths of 1 × 1 cm and excitation wavelengths (λ_{ex}) of 430 and 500 nm. All the compounds were dissolved in methanol with 0.1% trifluoroacetic acid; final concentration of compound was 33.3 μM. Spectra were corrected for background solvent emission. Chloroform (0.5%) was added to the sample of all-*trans*-retinal dimer-PE to ensure solubility.

3. Results

3.1. Fluorescence spectroscopy

Since RPE lipofuscin constituents are fluorescent compounds, we compared the emission spectra of all-*trans*-retinal dimer-PE, all-*trans*-retinal dimer-E and all-*trans*-retinal dimer with that of A2E. With excitation at 430 nm, the fluorescence of A2E and isoA2E had a relatively broad emission spectra with maxima at ~600 nm (Fig. 2A), as we have previously reported (Sparrow, Parish, Hashimoto, & Nakanishi, 1999). Excitation of all-*trans*-retinal dimer-PE and all-*trans*-retinal dimer-E at 500 nm, the wavelength corresponding to the absorbance maxima of these compounds, also resulted in an emission centered at approximately 600 nm but the

maxima were poorly defined and overall, the fluorescence emission was considerably weaker (Fig. 2B). On the other hand, unconjugated all-*trans*-retinal dimer displayed appreciable fluorescence when excited at 430 nm. Relative to A2E/isoA2E, the emission spectrum of unconjugated all-*trans*-retinal dimer was considerably blue-shifted, spectral width was reduced, fluorescence intensity was greater and peak emission occurred at approximately 510 nm.

3.2. Oxidation of A2E and all-trans-retinal dimer confers increased autofluorescence

A2E and all-*trans*-retinal dimer are both fluorescence compounds that serve as sensitizers in photooxidative processes (Ben-Shabat, Itagaki, et al., 2002; Kim, Jang, et al., 2007; Sparrow et al., 2002). Since the polyene chains of these compounds are oxidized during these photochemical reactions (Ben-Shabat, Itagaki, et al., 2002; Jang et al., 2005; Kim, Jang, et al., 2007), we were interested to examine the fluorescence characteristics of oxidized forms of A2E and all-*trans*-retinal dimer. Although we know from *in vitro* studies that the photooxidation of A2E can involve the incorporation of as many as nine oxygens into the retinoid-derived side-arms of the molecule with the formation of multiple oxygen-containing moieties (Ben-Shabat, Itagaki, et al., 2002; Jang et al., 2005; Kim, Jang, et al., 2007), because of the complexities of detection, we limited our investigation to mono- and bis-oxidized forms of A2E and all-*trans*-retinal dimer.

Chromatographic detection of A2E, isoA2E and oxidized forms of A2E with online monitoring of fluorescence and UV–visible absorbance are presented in Fig. 3. Here bisperoxy- and monoperoxy-A2E (Fig. 3A) were generated by incubating A2E with the singlet oxygen generator endoperoxide of 1,4-dimethylnaphthalene; bisfurano-A2E and monofurano-A2E (Fig. 3B) were produced by oxidation with MCPBA. On the C18 column, all of these oxidized forms of A2E exhibit shorter retention times than A2E because of increased polarity (Fig. 3A and B). As indicated by comparing the fluorescence (red) and absorbance (black) traces, the fluorescence intensities relative to absorbance (peak heights) were greater for mono- and bisperoxy-A2E than for A2E and isoA2E (Fig. 3A). Similar increases in the fluorescence intensity of mono- and bisfurano-A2E were observed when analyzing A2E samples oxidized by MCPBA (Fig. 3B).

Since we have previously illustrated the detection of photooxidized products of all-*trans*-retinal dimer in extracts of *Abca*4 null mutant mice (Kim, Jang, et al., 2007), we sought to provide similar evidence for the presence of photooxidized-A2E species in the mutant mouse eyecups (Fig. 3C). Overlay of the HPLC chromatograms generated with the (i) eyecup extract, (ii) peroxy-A2E (synthesized by incubating A2E with the singlet oxygen generator) and (iii) furano-A2E (synthesized by incubating A2E with MCPBA) revealed the expected oxidized-A2E species eluting earlier than A2E because of increased polarity. From this examination, it was also apparent that photooxidation is associated with hypsochromic shifts in absorbance (relative to A2E and isoA2E, λ_{max} = 335, 439; and 338, 428 nm, respectively) (Fig. 3C). These shifts are indicative of oxidation-associated loss of two double bonds in bisperoxy-A2E (λ_{max} = 290, 401 nm) and bisfurano-A2E (λ_{max} = 290, 402 nm) and loss of one double bond in monoperoxy-A2E and monofurano-A2E (λ_{max} = 282, 432 nm). Note that monoperoxy-A2E and monofurano-A2E can undergo an increase in fluorescence emission without a change in visible-spectrum absorbance. This is because the absorbance in the visible range is generated by the long arm of A2E while the first oxidation is always on the opposite (short) arm of A2E (Jang et al., 2005; Kim, Jang, et al., 2007). Since the absorbance in the visible range is similar for A2E and monofurano-A2E (Fig. 3B), we estimated the fluorescence efficiency per absorbed photon (calculated as fluorescence peak height/absorbance
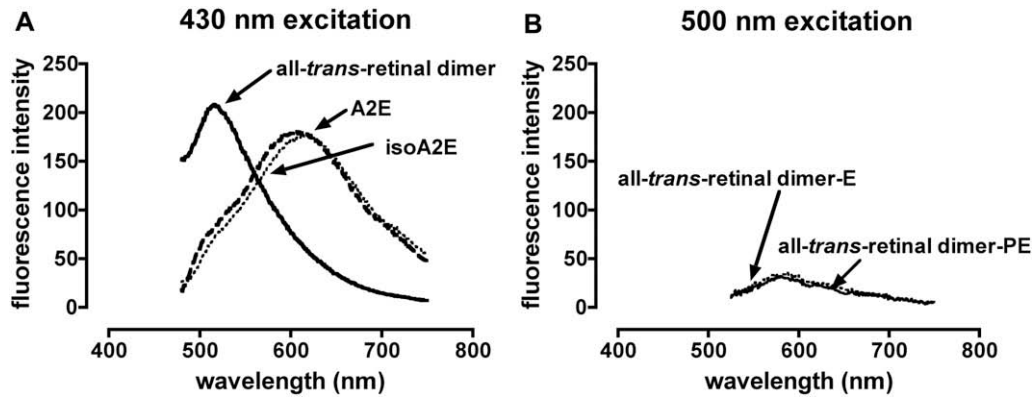
Fig. 2. Fluorescence emission spectra of A2E, isoA2E, all-*trans*-retinal dimer (A) and all-*trans-retinal* dimer-ethanolamine (all-*trans*-retinal dimer-E), all-*trans*-retinal dimer-phosphatidylethanolamine (all-*trans*-retinal *dimer*-PE) (B). Spectra were recorded at excitation wavelengths of 430 nm (A) and 500 nm (B). Fluorescence intensity is presented in arbitrary units.
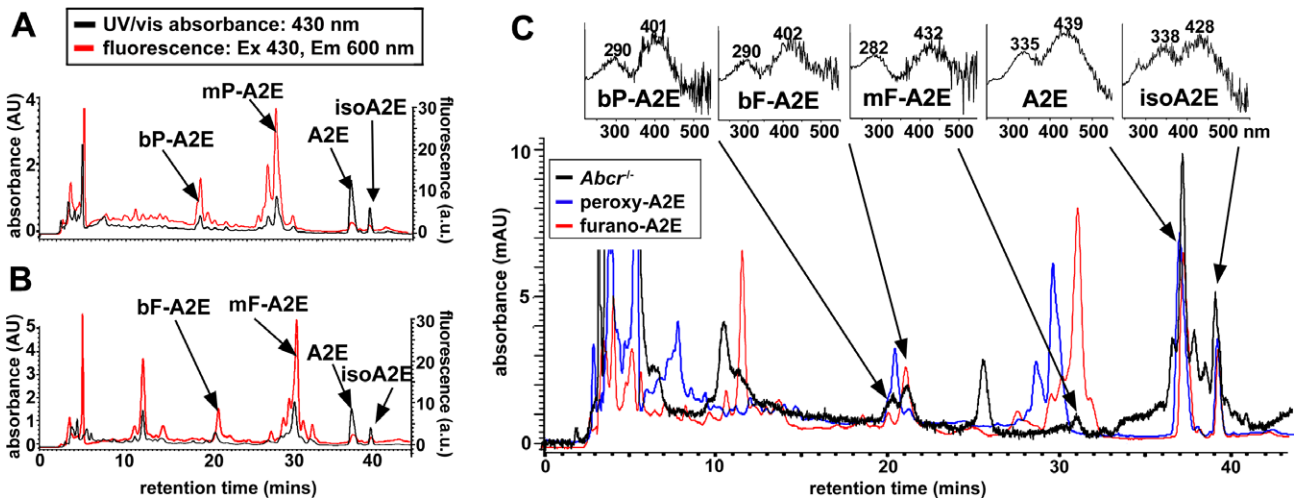

Fig. 3. Oxidation of A2E confers increased autofluorescence emission. (A) UV–visible absorbance and fluorescence detected in a mixture of A2E, isoA2E, monoperoxy-A2E and bisperoxy-A2E with separation by reverse-phase HPLC. Peroxy-A2E was generated by oxidation of A2E with endoperoxide of 1,4-dimethylnaphthalene. (B) UV–visible and fluorescence detected in a mixture of A2E, isoA2E, monofurano-A2E and bisfurano-A2E. Furano-A2E was generated by oxidation with *meta*-chloroperoxy-benzoic acid (MCPBA). AU, absorbance units; a.u., arbitrary units of fluorescence intensity. (C) HPLC chromatogram demonstrating the detection of oxidized forms of A2E in *Abca*4$^{-/-}$ mice eyes. Overlay of chromatograms generated with extract of *Abca*4$^{-/-}$ posterior eyecups (Rpe65 Leu-450; age 20 months; albino; 4 eyecups) (black) together with samples of peroxy-A2E (blue) and furano-A2E (red); 430 nm detection. *Top insets*, UV–visible absorbance of A2E, isoA2E and oxidized forms of A2E: bisperoxy-A2E (bP-A2E), bisfurano-A2E (bF-A2E), monofurano-A2E (mF-A2E).

peak height at 430 nm irradiation) and found this to be 0.28 for A2E and 2.86 for furano-A2E.

Chromatographic separations of mixtures of all-*trans*-retinal dimer and oxidized-all-*trans*-retinal dimer, with online monitoring of fluorescence emission and UV–visible absorbance, are shown in Fig. 4. As noted above, bisperoxy- and monoperoxy-all-*trans*-retinal dimer (Fig. 4A) were generated by incubating all-*trans*-retinal dimer with the singlet oxygen generator endoperoxide of 1,4-dimethylnaphthalene and bisfurano-all-*trans*-retinal dimer and mono-furano-all-*trans*-retinal dimer (Fig. 4B) were produced by oxidation with MCPBA. The oxidized forms of all-*trans*-retinal dimer eluted ahead of the parent compound due to decreased hydrophobicity. Moreover, for bisfurano-all-*trans*-retinal dimer and particularly for bisperoxy-all-*trans*-retinal dimer, fluorescence peak height (red) was greater than absorbance peak height (black); this difference is readily visible when compared to the absorbance and fluorescence traces of all-*trans*-retinal dimer (un-oxidized) and is indicative of oxidation-associated enhanced fluorescence.

On the basis of UV–visible absorbance spectra and retention times that corresponded to the authentic standards, photooxidized

forms of all-*trans*-retinal dimer could be detected in chloroform/methanol extracts of eyecups harvested from *Abca*4$^{-/-}$ mice. Shown in Fig. 4C, is a reverse-phase HPLC chromatogram generated with absorbance and fluorescence monitoring online; fluorescence and absorbance are presented as overlapping traces. Note that for bisperoxy-all-*trans*-retinal dimer and bisfurano-all-*trans*-retinal dimer, the height of the fluorescence peak is increased relative to the absorbance peak. In addition, hypsochromic shifts in absorbance occur due to oxidation-associated loss of double bonds.

3.3. Detection of oxidized all-trans-retinal dimer in human RPE

Because in *in vitro* experiments, unconjugated all-*trans*-retinal dimer can serve as both a photosensitizer for and quencher of singlet oxygen (Kim, Jang, et al., 2007), we sought to provide evidence for these photochemical processes in the human eye. To this end we isolated RPE from human donor eyes and analyzed the chloroform–methanol extractable pigments in these tissues. As shown in the chromatogram in Fig. 5, analysis of the RPE extracts with a reverse-phase C18 column and monitoring at 430 nm, lead to the
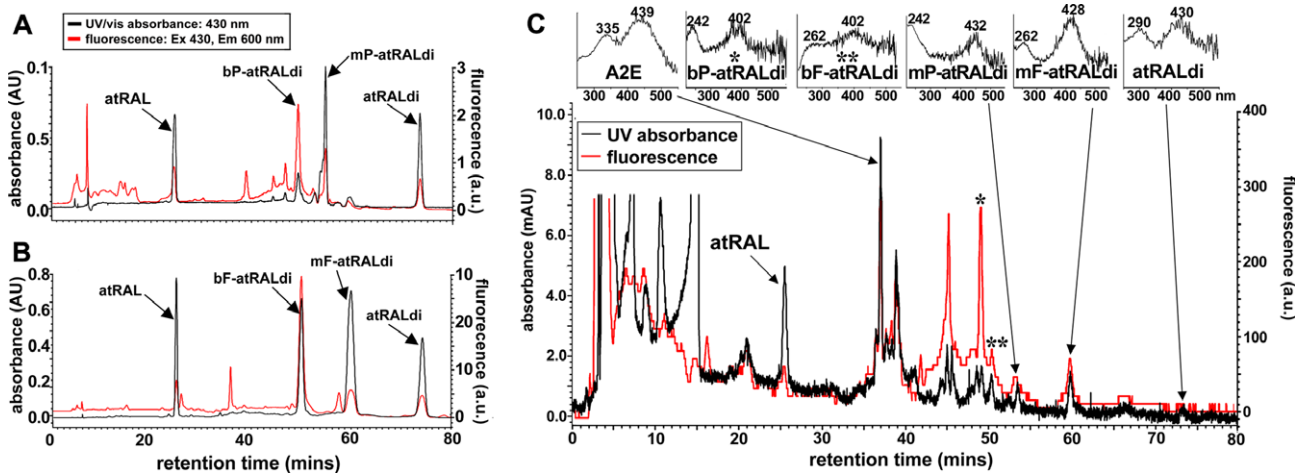
Fig. 4. Fluorescence and absorbance monitoring of all-*trans*-retinal dimer and oxidized all-*trans*-retinal dimer. (A) UV–visible and fluorescence intensity detected in a mixture of all-*trans*-retinal dimer (atRALdi), monoperoxy-all-*trans*-retinal dimer (mP-atRALdi) and bisperoxy-all-*trans*-retinal dimer (bP-atRALdi) with separation by reverse-phase HPLC. Peroxy-all-*trans*-retinal dimer was generated by oxidation with endoperoxide of 1,4-dimethylnaphthalene. (B) UV–visible and fluorescence detection of a mixture of all-*trans*-retinal dimer, mono-furano-all-*trans*-retinal dimer (mF-atRALdi) and bisfurano-all-*trans*-retinal dimer (bF-atRALdi). Furano-all-*trans*-retinal dimer was generated by oxidation with *meta*-chloroperoxy-benzoic acid (MCPBA). AU, absorbance units; a.u., arbitrary units of fluorescence intensity. (C) UV–visible and fluorescence intensity recorded during HPLC separation of pigments in an extract of *Abca*4[−/−] posterior eyecups (Rpe65 Leu-450; albino; age 5.5 months; 4 eyecups). *Top insets*, UV–visible absorbance of A2E, all-*trans*-retinal dimer and oxidized forms of all-*trans*-retinal dimer: bisperoxy-all-*trans*-retinal dimer (bP-atRALdi), bisfurano-all-*trans*-retinal dimer (bF-atRALdi), monoperoxy-all-*trans*-retinal dimer (mP-atRALdi), mono-furano-all-*trans*-retinal dimer (mF-atRALdi).

detection of A2E, isoA2E and other minor *cis*-isomers of A2E (Ben-Shabat, Parish, et al., 2002; Parish et al., 1998) that have been shown to interconvert with A2E *in vivo* (Fig. 5). By observing for co-elution with synthetic standards, peaks attributable to all-*trans*-retinal dimer and all-*trans*-retinal dimer-PE were also observed. Similarly, amongst the peaks eluting earlier than all-*trans*-retinal dimer, we identified bisperoxy-all-*trans*-retinal dimer, bisfurano-all-*trans*-retinal dimer and mono-furano-all-*trans*-retinal dimer. Elution earlier than all-*trans*-retinal dimer is to be expected of oxidized products having increased polarity.

3.4. Oxidized all-trans-retinal dimer is more abundant than all-trans-retinal dimer

We also compared the amount of all-*trans*-retinal dimer and oxidized all-*trans*-retinal dimer in *Abca*4 null mutant versus wild-type mice (Fig. 6). The levels of all-*trans*-retinal dimer in *Abca*4[−/−] mice were modestly greater than in *Abca*4[+/+], with the magnitude of the difference between 2-fold at 8 months of age. The amount of oxidized all-*trans*-retinal dimer was even more pronounced; oxidized all-*trans*-retinal dimer was almost 3-fold higher in the *Abca*4[−/−] mice. In both wild-type and *Abca*4[−/−] mice, the levels of oxidized all-*trans*-retinal dimer exceeded the amounts of all-*trans*-retinal dimer.

4. Discussion

A2E/isoA2E and the all-*trans*-retinal dimer series of compounds are all derived from reactions of all-*trans*-retinal; accordingly they present with bisretinoid structures. For all of these compounds the two-armed polyene structures ending in β-ionone rings provide the extended conjugation systems that confer absorbance maxima in the visible range of the spectrum: all-*trans*-retinal dimer-PE/all-*trans*-retinal dimer-E, λ_{max} ∼510 nm; all-*trans*-retinal dimer, λ_{max} ∼430 nm; A2E, λ_{max} ∼439 nm. These absorbance differences are reflected in the colors of the chromophores in solution: A2E/iso-A2E is yellow, all-*trans*-retinal dimer-PE/ all-*trans*-retinal dimer-E is violet. When excited at wavelengths that approximate their absorbance maxima, A2E/isoA2E and all-*trans*-retinal dimer-PE/

all-*trans*-retinal dimer-E exhibit orange fluorescence while the fluorescence of all-*trans*-retinal dimer is blue-shifted. When excited at their absorbance maxima (510 nm), all-*trans*-retinal dimer-PE/all-*trans*-retinal dimer-E are considerably less fluorescent than A2E.

Comparison of the emission spectra of A2E with emission generated *in vivo* from fundus autofluorescence reveals similarly shaped spectra with maxima at approximately 600 nm (excitation 430 nm) (Delori, Keilhauer, Sparrow, & Staurenghi, 2007). However, when the excitation spectra are considered, the spectrum elicited from A2E is narrower and is shifted towards shorter wavelengths compared with those from the fundus. While this difference is consistent with the fact that A2E is not the only lipofuscin fluorophore responsible for fundus autofluorescence, whether the compounds of the all-*trans*-retinal dimer series or A2-DHP-PE can account for these differences, has not been determined. What is of interest however, is the report that an age-associated blue-shift in the emission spectra occurs that is indicative of a relative increase in fundus autofluorescence in the 500–540 nm range (Delori et al., 2007). An increase in oxidized all-*trans*-retinal dimer could provide an explanation.

We have shown here that oxidized forms of A2E and all-*trans*-retinal dimer exhibit hypsochromic absorbance shifts reflecting oxidation-associated loss of double bond conjugations. For every double bond lost, a shift of approximately 30 nm results. It should be noted however, that A2E and all-*trans*-retinal dimer present with two side-arms, each of which produces an absorbance maxima. For instance for A2E, the 439 nm absorbance maxima is generated by the long arm and a 335 nm absorbance by the short arm. This situation allows us to determine on which arm an oxidation-associated loss of double bond conjugation occurs. These sites of photooxidation also serve as loci for molecular cleavage, particularly at positions of singlet oxygen addition (Sparrow, Yanase, Siegel and Wu, unpublished observation). Moreover, our previous experimental findings are consistent with a scenario whereby the bisretinoid fragments resulting from photooxidation-associated cleavage diffuse inside and outside the cell (Sparrow et al., 2003; Sparrow, Zhou, & Cai, 2003; Zhou et al., 2005; Zhou, Jang, Kim, & Sparrow, 2006; Zhou, Kim, Westlund, & Sparrow, 2009). Consequently, the fraction of oxidized-A2E and oxidized-all-*trans*-retinal
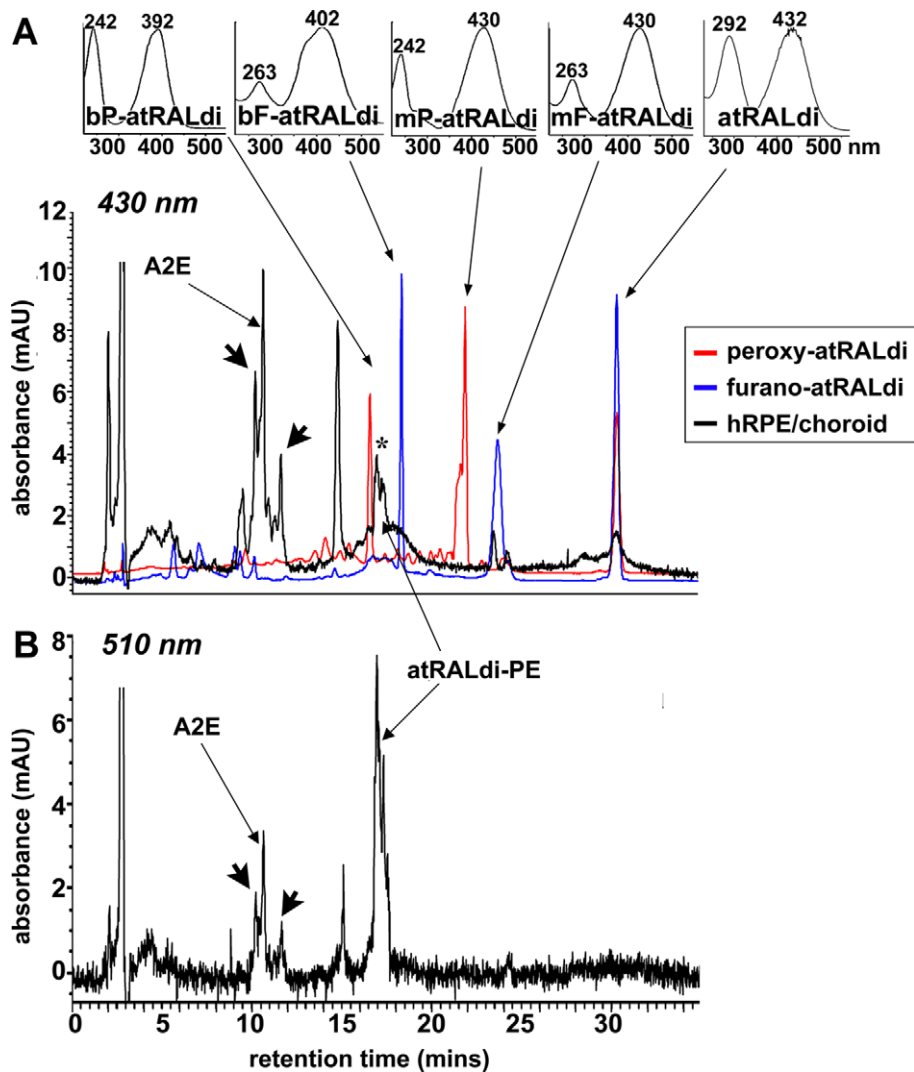
Fig. 5. Detection of oxidized forms of all-*trans*-retinal dimer in hydrophobic extract of isolated human RPE/choroid (hRPE/choroid); 64-year-old donor. Reverse-phase C18 column. (A) Overlay of reverse-phase HPLC chromatograms (monitoring at 430 nm) generated when HPLC injectant was extract of hRPE/choroid (black), reaction mixture of all-*trans*-retinal dimer with MCPBA (blue), or reaction mixture of all-*trans*-retinal dimer with endoperoxide of 1,4-dimethylnaphtalene (red). *Top insets*, UV–visible absorbance spectra of all-*trans*-retinal dimer (atRALdi) and oxidized forms of all-*trans*-retinal dimer: mono-furano all-*trans*-retinal dimer (mF-atRALdi), bisfurano-all-*trans*-retinal dimer (bF-atRALdi), monoperoxy-all-*trans*-retinal dimer (mP-atRALdi), bisperoxy-all-*trans*-retinal dimer. (B) Monitoring at 510 nm; the peak attributable to all-*trans*-retinal dimer-PE is readily distinguished with monitoring at the absorbance maximum of this compound. *Arrow-heads*, isomers of A2E; *A2-dihydropyridine-phosphatidylethanolamine (A2-DHP-PE). (For interpretation of the references to color in this figure legend, the reader is referred to the web version of this article.)

dimer that we observed in the tissue extracts shown here, is unlikely to be stable over time. Indeed photooxidation-associated degradation of these bisretinoids probably causes a loss of this material even as newly formed bisretinoid is being deposited. When considering the levels of individual bisretinoid lipofuscin compounds, for instance A2E versus the compounds of the all-*trans*-retinal-dimer series, one should also bear in mind that the rates of photodegradation can vary. Photodegradation of all-*trans*-retinal dimer is likely to be more robust than for A2E.

The autofluorescence signal emanating from the fundus is not distributed uniformly. Fundus autofluorescence images from subjects with healthy retinal status, exhibit low levels of autofluorescence at the fovea, in part because lipofuscin may be less abundant there but also because of macular pigment absorption and attenuation of the signal by RPE melanin (Delori et al., 2007). Outside the fovea fundus autofluorescence increases gradually to a maximum at an eccentricity of 7–13° and then declines toward the periphery. Superimposed on this normal topographic distribution, disease-related abnormalities in fundus autofluorescence signaling can be detected. For instance, absence or minimal fundus autofluores-

cence is attributable to RPE atrophy. Disease-associated increases in fundus autofluorescence intensity, both focal increases and those present at the borders of atrophy, are usually attributable to an increased content of lipofuscin or to displacement or clumping of lipofuscin-laden RPE (Holz, Bellman, Staudt, Schutt, & Volcker, 2001; Holz et al., 1999). Here we show that oxidation of A2E and all-*trans*-retinal dimer can also produce fluorescence of heightened intensity. When the oxidation occurs on the short arm of the molecule, the increase in fluorescence emission occurs without a change in the absorbance maximum in the visible range of the spectrum. We have previously shown that all-*trans*-retinal dimer is a more efficient generator of singlet oxygen than is A2E; in addition, all-*trans*-retinal dimer exhibits more pronounced singlet oxygen reaction rates (Kim, Jang, et al., 2007). These findings are consistent with the current observation that, based on HPLC peak areas, the levels of oxidized all-*trans*-retinal dimer are greater than the levels of the parent compound (all-*trans*-retinal dimer).

In summary, the identification and characterization of the bisretinoid components of RPE lipofuscin, including those generated by photooxidation, is fundamentally important, in the least be-
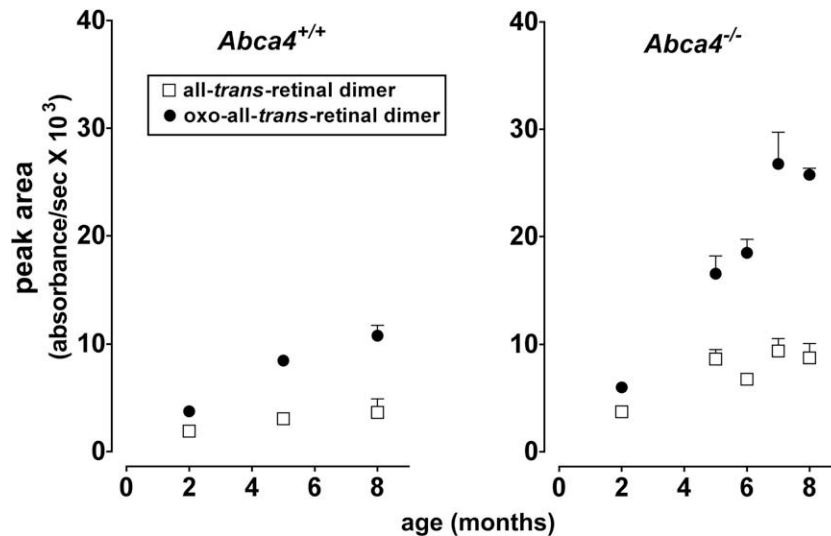
Fig. 6. Levels of all-*trans*-retinal dimer and oxidized all-*trans*-retinal dimer in age-matched wild-type ($Abca4^{+/+}$) mice and $Abca4$ null mutant ($Abca4^{-/-}$). The lipofuscin pigments were quantified from reverse-phase HPLC chromatograms with 430 nm detection; levels of oxidized all-*trans*-retinal dimer (oxo-all-*trans*-retinal dimer) were determined as the sum of mono-furano-all-*trans*-retinal dimer and monoperoxy-all-*trans*-retinal dimer. Mice were albino and homozygous for Rpe65 Leu-450. Mean ± SEM, 4 eyes per sample.

cause these compounds have different properties and can be expected to impact on RPE cells in a variety of ways (Sparrow, 2007). Improved understanding of the constituents also increases awareness of the total burden placed on the RPE cell by the deposition of this retinoid-derived material. The results reported here have practical implications for methods that rely on fluorescence intensity to measure RPE lipofuscin as therapeutic endpoint.

Acknowledgments

References

Ben-Shabat, S., Itagaki, Y., Jockusch, S., Sparrow, J. R., Turro, N. J., & Nakanishi, K. (2002a). Formation of a nona-oxirane from A2E, a lipofuscin fluorophore related to macular degeneration, and evidence of singlet oxygen involvement. *Angewandte Chemie International Edition, 41*(5), 814–817.

Ben-Shabat, S., Parish, C. A., Vollmer, H. R., Itagaki, Y., Fishkin, N., Nakanishi, K., et al. (2002b). Biosynthetic studies of A2E, a major fluorophore of RPE lipofuscin. *Journal of Biological Chemistry, 277*(9), 7183–7190.

Delori, F. C., Dorey, C. K., Staurenghi, G., Arend, O., Goger, D. G., & Weiter, J. J. (1995). In vivo fluorescence of the ocular fundus exhibits retinal pigment epithelium lipofuscin characteristics. *Investigative Ophthalmology and Visual Science, 36*(3), 718–729.

Delori, F. C., Goger, D. G., & Dorey, C. K. (2001). Age-related accumulation and spatial distribution of lipofuscin in RPE of normal subjects. *Investigative Ophthalmology and Visual Science, 42*, 1855–1866.

Delori, F. C., Keilhauer, C., Sparrow, J. R., & Staurenghi, G. (2007). Origin of fundus autofluorescence. In F. G. Holz, S. Schmitz-Valckenberg, R. F. Spaide, & A. C. Bird (Eds.), *Atlas of fundus autofluorescence imaging* (pp. 17–29). Berlin, Heidelberg: Springer-Verlag.

Delori, F. C., Staurenghi, G., Arend, O., Dorey, C. K., Goger, D. G., & Weiter, J. J. (1995). In vivo measurement of lipofuscin in Stargardt's disease – Fundus flavimaculatus. *Investigative Ophthalmology and Visual Science, 36*(11), 2327–2331.

Eldred, G. E., & Katz, M. L. (1988). Fluorophores of the human retinal pigment epithelium: Separation and spectral characterization. *Experimental Eye Research, 47*(1), 71–86.

Eldred, G. E., & Lasky, M. R. (1993). Retinal age pigments generated by self-assembling lysosomotropic detergents. *Nature, 361*(6414), 724–726.

Fishkin, N., Pescitelli, G., Sparrow, J. R., Nakanishi, K., & Berova, N. (2004). Absolute configurational determination of an all-trans-retinal dimer isolated from photoreceptor outer segments. *Chirality, 16*, 637–641.

Fishkin, N., Sparrow, J. R., Allikmets, R., & Nakanishi, K. (2005). Isolation and characterization of a retinal pigment epithelial cell fluorophore: An all-trans-retinal dimer conjugate. *Proceedings of the National Academy of Sciences of the United States of America, 102*(20), 7091–7096.

Holz, F. G., Bellman, C., Staudt, S., Schutt, F., & Volcker, H. E. (2001). Fundus autofluorescence and development of geographic atrophy in age-related macular degeneration. *Investigative Ophthalmology and Visual Science, 42*(5), 1051–1056.

Holz, F. G., Bellmann, C., Margaritidis, M., Schutt, F., Otto, T. P., & Volcker, H. E. (1999). Patterns of increased in vivo fundus autofluorescence in the junctional zone of geographic atrophy of the retinal pigment epithelium associated with age-related macular degeneration. *Graefe's Archive for Clinical and Experimental Ophthalmology, 237*, 145–152.

Jang, Y. P., Matsuda, H., Itagaki, Y., Nakanishi, K., & Sparrow, J. R. (2005). Characterization of peroxy-A2E and furan-A2E photooxidation products and detection in human and mouse retinal pigment epithelial cells lipofuscin. *Journal of Biological Chemistry, 280*, 39732–39739.

Kim, S. R., Fishkin, N., Kong, J., Nakanishi, K., Allikmets, R., & Sparrow, J. R. (2004). The Rpe65 Leu450Met variant is associated with reduced levels of the RPE lipofuscin fluorophores A2E and iso-A2E. *Proceedings of the National Academy of Sciences of the United States of America, 101*(32), 11668–11672.

Kim, S. R., He, J., Yanase, E., Jang, Y. P., Berova, N., Sparrow, J. R., et al. (2007a). Characterization of dihydro-A2PE: An intermediate in the A2E biosynthetic pathway. *Biochemistry, 46*, 10122–10129.

Kim, S. R., Jang, Y. P., Jockusch, S., Fishkin, N. E., Turro, N. J., & Sparrow, J. R. (2007b). The all-trans-retinal dimer series of lipofuscin pigments in retinal pigment epithelial cells in a recessive Stargardt disease model. *Proceedings of the National Academy of Sciences of the United States of America, 104*, 19273–19278.

Kim, S. R., Jockusch, S., Itagaki, Y., Turro, N. J., & Sparrow, J. R. (2008). Mechanisms involved in A2E oxidation. *Experimental Eye Research.*

Liu, J., Itagaki, Y., Ben-Shabat, S., Nakanishi, K., & Sparrow, J. R. (2000). The biosynthesis of A2E, a fluorophore of aging retina, involves the formation of the precursor, A2-PE, in the photoreceptor outer segment membrane. *Journal of Biological Chemistry, 275*(38), 29354–29360.

Lois, N., Holder, G. E., Bunce, C. V., Fitzke, F. W., & Bird, A. C. (2001). Phenotypic subtypes of Stargardt macular dystrophy – fundus flavimaculatus. *Archives of Ophthalmology, 119*, 359–369.

Lois, N., Owens, S. L., Coco, R., Hopkins, J., Fitzke, F. W., & Bird, A. C. (2002). Fundus autofluorescence in patients with age-related macular degeneration and high risk of visual loss. *American Journal of Ophthalmology, 133*, 341–349.

Parish, C. A., Hashimoto, M., Nakanishi, K., Dillon, J., & Sparrow, J. R. (1998). Isolation and one-step preparation of A2E and iso-A2E, fluorophores from human retinal pigment epithelium. *Proceedings of the National Academy of Sciences of the United States of America, 95*(25), 14609–14613.

Radu, R. A., Han, Y., Bui, T. V., Nusinowitz, S., Bok, D., Lichter, J., et al. (2005). Reductions in serum vitamin A arrest accumulation of toxic retinal fluorophores: A potential therapy for treatment of lipofuscin-based retinal diseases. *Investigative Ophthalmology and Visual Science, 46*, 4393–4401.

Sakai, N., Decatur, J., Nakanishi, K., & Eldred, G. E. (1996). Ocular age pigment "A2E": An unprecedented pyridinium bisretinoid. *Journal of the American Chemical Society, 118*, 1559–1560.

Schmitz-Valckenberg, S., Bultmann, S., Dreyhaupt, J., Bindewald, A., Holz, F. G., & Rohrschneider, K. (2004). Fundus autofluorescence and fundus perimetry in the junctional zone of geographic atrophy in patients with age-related macular degeneration. *Investigative Ophthalmology and Visual Science, 45*, 4470–4476.

Scholl, H. P. N., Bellmann, C., Dandekar, S. S., Bird, A. C., & Fitzke, F. W. (2004). Photopic and scotopic fine matrix mapping of retinal areas of increased fundus autofluorescence in patients with age-related maculopathy. *Investigative Ophthalmology and Visual Science, 45*, 574–583.

Sparrow, J. R. (2007). Lipofuscin of the retinal pigment epithelium. In F. G. Holz, S. Schmitz-Valckenberg, R. F. Spaide, & A. C. Bird (Eds.), *Atlas of autofluorescence imaging* (pp. 3–16). Heidelberg: Springer.

Sparrow, J. R., Nakanishi, K., & Parish, C. A. (2000). The lipofuscin fluorophore A2E mediates blue light-induced damage to retinal pigmented epithelial cells. *Investigative Ophthalmology and Visual Science, 41*(7), 1981–1989.

Sparrow, J. R., Parish, C. A., Hashimoto, M., & Nakanishi, K. (1999). A2E, a lipofuscin fluorophore, in human retinal pigmented epithelial cells in culture. *Investigative Ophthalmology and Visual Science, 40*(12), 2988–2995.

Sparrow, J. R., Vollmer-Snarr, H. R., Zhou, J., Jang, Y. P., Jockusch, S., Itagaki, Y., et al. (2003). A2E-epoxides damage DNA in retinal pigment epithelial cells. Vitamin E and other antioxidants inhibit A2E-epoxide formation. *Journal of Biological Chemistry, 278*, 18207–18213.

Sparrow, J. R., Zhou, J., Ben-Shabat, S., Vollmer, H., Itagaki, Y., & Nakanishi, K. (2002). Involvement of oxidative mechanisms in blue light induced damage to A2E-laden RPE. *Investigative Ophthalmology and Visual Science, 43*(4), 1222–1227.

Sparrow, J. R., Zhou, J., & Cai, B. (2003). DNA is a target of the photodynamic effects elicited in A2E-laden RPE by blue light illumination. *Investigative Ophthalmology and Visual Science, 44*, 2245–2251.

Turro, N. J., Chow, M.-F., & Rigaudyo, J. (1981). Mechanism of thermolysis of endoperoxides of aromatic compounds. Activation parameters, magnetic field, and magnetic isotope effects. *Journal of the American Chemical Society, 103*, 7218–7222.

von Ruckmann, A., Fitzke, F. W., & Bird, A. C. (1997). In vivo fundus autofluorescence in macular dystrophies. *Archives of Ophthalmology, 115*, 609–615.

von Rückmann, A., Fitzke, F. W., & Bird, A. C. (1997). Fundus autofluorescence in age-related macular disease imaged with a laser scanning ophthalmoscope. *Investigative Ophthalmology and Visual Science, 38*(2), 478–486.

Wu, Y., Fishkin, N. E., Pande, A., Pande, J., & Sparrow, J. R. (2009). Novel lipofuscin bisretinoids prominent in human retina and in a model of recessive Stargardt disease. *Journal of Biological Chemistry, 284*, 20155–20166.

Zhou, J., Cai, B., Jang, Y. P., Pachydaki, S., Schmidt, A. M., & Sparrow, J. R. (2005). Mechanisms for the induction of HNE- MDA- and AGE-adducts, RAGE and VEGF in retinal pigment epithelial cells. *Experimental Eye Research, 80*, 567–580.

Zhou, J., Jang, Y. P., Kim, S. R., & Sparrow, J. R. (2006). Complement activation by photooxidation products of A2E, a lipofuscin constituent of the retinal pigment epithelium. *Proceedings of the National Academy of Sciences of the United States of America, 103*, 16182–16187.

Zhou, J., Kim, S. R., Westlund, B. S., & Sparrow, J. R. (2009). Complement activation by bisretinoid constituents of RPE lipofuscin. *Investigative Ophthalmology and Visual Science, 50*, 1392–1399.